Pergamon

0306-4522(95)00463-7

Neuroscience Vol. 71, No. 2, pp. 489–505, 1996
Elsevier Science Ltd

0306-4522/96 $15.00 + 0.00

ULTRASTRUCTURAL LOCALIZATION OF B-50/GROWTH-ASSOCIATED PROTEIN-43 TO ANTEROGRADELY TRANSPORTED SYNAPTOPHYSIN-POSITIVE AND CALCITONIN GENE-RELATED PEPTIDE-NEGATIVE VESICLES IN THE REGENERATING RAT SCIATIC NERVE

P. VERKADE,* A. J. VERKLEIJ,† W. G. ANNAERT,‡ W. H. GISPEN* and A. B. OESTREICHER*§

*Rudolf Magnus Institute for Neurosciences, University of Utrecht, Universiteitsweg 100, 3584CG, Utrecht, The Netherlands

†Institute of Biomembranes, University of Utrecht, Padualaan 8, 3584CH Utrecht, The Netherlands

‡HHMI, Yale University School of Medicine, BCMM, 295 Congress Avenue, New Haven, CT 06536-0812, U.S.A.

Abstract—The growth-associated protein-43/B-50 (B-50/GAP-43) is conveyed from the neuronal soma into the axon by fast axonal transport and moved to the nerve terminal. To visualize and determine the type of vesicles by which B-50/GAP-43 is anterogradely transported in the regenerating rat sciatic nerve, we have investigated Lowicryl HM20 embedded nerve pieces dissected from the proximal side of a collection ligature. Ultrastructurally, numerous vesicular profiles of various sizes, tubules and mitochondria were seen to accumulate proximal to the collection ligature. Both, in unmyelinated and myelinated axons, B-50/GAP-43 immunoreactivity was associated with vesicular profiles which had a diameter of 50 nm. A fraction of the B-50/GAP-43 label co-localized with the small vesicle marker synaptophysin. Co-localization of B-50/GAP-43 was not detected with the large dense-core vesicle marker calcitonin gene-related peptide.

These results indicate that, in rat sciatic nerve axons, B-50/GAP-43 is anterogradely transported in small 50 nm vesicles of the constitutive pathway. These transport vesicles were distinguished in two types. We suggest that one type carrying, both, B-50 GAP-43 and synaptophysin has as destination the nerve terminal, whereas the second type, which only contains B-50/GAP-43 and no synaptophysin, may be primarily targeted to the axolemma for local membrane fusion.

Key words: axonal transport, ligation, double immunolabelling, electron microscopy, membrane fusion, vesicle size.

The growth-associated protein B-50/GAP-43 is generally regarded as a plasticity marker for neurite outgrowth, since it is highly expressed during nervous tissue development and regeneration.[46,53] There is evidence that B-50/GAP-43 plays a crucial role in neuritogenesis, axonal regeneration, synaptic plasticity and neurotransmission.[20,46,53] In the adult CNS B-50/GAP-43 may be involved in neurotransmitter release.[25] During embryonic development of transgenic mice lacking B-50/GAP-43, retinal axons have been shown to be trapped in the optic chiasm unable to navigate for some days beyond this decision point,[52] indicating that at certain critical time points and places B-50/GAP-43 may be required for neurite extension or growth cone formation. A comparable deficiency has been reported for chick dorsal root ganglion neurons cultured *in vitro* and depleted of B-50/GAP-43.[1] The neurons displayed poor adherence to the substratum and unstable lamellar extensions of growth cones. Long-lasting overexpression of B-50/GAP-43 in non-neuronal cells in culture induces formation of neurite-like extensions.[62] Despite extensive studies the exact function of B-50/GAP-43 in each of these processes is still unknown.

During the development of the nervous system high B-50/GAP-43 mRNA and protein levels are found in most brain areas.[14,28,37] After target innervation levels of B-50/GAP-43 are down regulated. Certain "plastic" areas in the adult CNS, such as the associative cortex and the hippocampus, retain appreciable expression of B-50/GAP-43.[4,33]

§To whom correspondence should be addressed.

Abbreviations: CGRP, calcitonin gene-related peptide; DRG, dorsal root ganglion; LDCV, large dense-cored vesicles; GAP, growth-associated protein; PBS, phosphate-buffered saline; PFA, paraformaldehyde; PNS, peripheral nervous system; p38, synaptophysin; SSV, small synaptic vesicles; STV, small transport vesicles.

In the adult peripheral nervous system (PNS), expression of B-50/GAP-43 is relatively low compared with that of the CNS.[54,63,64] However, following peripheral nerve damage, a rapid induction of the B-50/GAP-43 expression (mRNA and protein) has been reported in motor neurons and dorsal root ganglion (DRG) neurons.[10,27,57] Axonal regeneration is initiated close to the peripheral lesion site. B-50/GAP-43 is enriched in regrowing sprouts distal to a crush of the rat sciatic nerve,[54,63] but also in the axons proximal to the crush.[64] In unmyelinated axons of the rat sciatic nerve, B-50/GAP-43 is found predominantly associated with the axolemma.[64] Schwann cells distal to the nerve lesion react to the loss of contact with the axons, by changing their program of protein expression, including up-regulation of the B-50/GAP-43 expression.[11,45,56,66]

During axon outgrowth, remodelling of nerve endings, neurotransmission and nerve regeneration, the expression of proteins required for membrane expansion is up-regulated. The proteins are synthesized predominantly in the neuronal cell body and are moved out by fast axonal transport to the axolemma, the growth cone or axon terminal.[39] For fast anterograde transport, proteins are packaged in the trans-Golgi network into, at least, two types of membrane-bounded vesicles;[12,16] the large dense-cored vesicles (LDCV) and small transport vesicles (STV). STV are constitutive organelles continuously delivering new membrane substances to the plasma membrane. Other components, such as, e.g. synaptophysin (p38)—a transmembrane protein of synaptic vesicles[29,30,65]—are recycled via an early endosomal compartment into small synaptic vesicles.[42] The intra-axonal transport operates in anterograde and retrograde directions. B-50/GAP-43 is conveyed by fast anterograde axonal transport[5,6,27,31,48,49,54] attached to vesicles by palmitoylation of its *N*-terminal domain.[36,47] In the rat sciatic nerve, B-50/GAP-43[35,54] and synaptophysin[13] are also translocated retrogradely.

In this study, we investigated whether membrane-bounded organelles carrying B-50/GAP-43 immunoreactivity can be detected and characterized as transport vesicles of the anterograde axonal transport in the regenerating sciatic nerve of the adult rat, using synaptophysin and calcitonin gene-related peptide (CGRP) as markers for vesicles in transport. The retrograde transport was excluded from this study. We have performed an ultrastructural morphometric and immunogold double labelling study of B-50/GAP-43 in the nerve region located proximal to a collection ligature which was placed on a regenerating rat sciatic nerve.

EXPERIMENTAL PROCEDURES

Animals and surgical procedures

Animal experiments were carried out according to protocols approved by the Animal Welfare Officer of the University of Utrecht. Adult male Wistar rats (body weight 200–250 g) under Hypnorm anaesthesia (Janssen Pharmaceutica, Tilburg, NL. 0.05 ml Hypnorm/100 g body weight, Hypnorm contains 10 mg fluanison and 0.315 mg fentanylcitrate per ml) were subjected to an unilateral crush of the sciatic nerve 27 mm distal from the sciatic notch.[17] Seven days after the crush, the animals were again anaesthetized and the sciatic nerve was exposed. A collection ligature was placed 1 cm proximal to the crush site, sutured and the wound was closed. Six hours later, the rats ($n = 2$) were killed by anaesthesia with an overdose Hypnorm (0.5 ml Hypnorm/100 g body weight) and fixed by intracardiac perfusion. The perfusion was performed with 100 ml of saline (0.15 M NaCl), followed by 300 ml of 4% paraformaldehyde (PFA, Merck, Darmstadt, Germany) and 2% glutaraldehyde (Merck, Darmstadt, Germany) in phosphate-buffered saline (PBS, 0.1 M phosphate buffer at pH 7.4, containing 150 mM NaCl). The ligated sciatic nerve was carefully dissected. The nerve segment 0–2 mm proximal to the collection ligature, was sampled. The nerve pieces were kept in the fixative overnight and stored in 1% PFA in PBS at 4°C.

Primary antibodies

An affinity purified polyclonal antibody to B-50/GAP-43,[40,60,61] designated 8613 was used in a dilution of 1:100.[64] A polyclonal antibody to CGRP (Peninsula, RAS 6009-N, CA, U.S.A.) was used in a dilution of 1:500. An affinity purified polyclonal antibody to synaptophysin (p38) was used in a dilution of 1:200.[2]

The specificity of the immunolabelling of B-50/GAP-43 was verified by preabsorption of the primary antibody with bovine B-50/GAP-43.[64] The controls were negative.

Immunogold labelling of ultrathin nerve sections

Perfusion fixed material was freeze-substituted to Lowicryl HM20 as described previously.[60,61,64] Longitudinal ultrathin (50–70 nm) sections were cut, collected and immunolabelled as previously described.[61,64] The complete procedure was carried out at room temperature and all solutions were made in tri-distilled water. In short, the sections were blocked and then incubated overnight with primary antibodies diluted in a humid chamber. After rinsing, the sections were incubated with either 1 or 10 nm gold particles attached to anti-rabbit immunoglobulins (Aurion, Wageningen, The Netherlands). The sections were rinsed and postfixed. In order to reveal the 1 nm gold particles attached to the complex, the particles were silver enhanced according to the procedure of Danscher,[15] and after 20 min the sections were thoroughly washed.

After single immunolabelling, sections were contrasted with uranyl acetate and lead citrate.

For double immunolabelling,[60] the first primary antibody was detected by 1 nm gold particles coated on a secondary antibody and subsequent silver enhancement. After the silver enhancement the sections were thoroughly rinsed, and the complete procedure for immunolabelling by a second primary antibody was repeated. In this new round of immunolabelling (second step), the second primary antibody was detected by a secondary antibody attached to 10 nm gold particles. After postfixation the sections were contrasted. Finally, sections were examined in a Philips CM10 electron microscope.

Two different rabbit polyclonal antibodies were used in the two-step immunolabelling procedure. The silver precipitate produced by the silver enhancement covers the primary and secondary antibody of the first immunolabelling step and prevents cross-reactivity between the first and the second immunolabelling step. Cross-reactivity did not occur when the detection of the primary antibodies was performed with 1 nm gold particles followed by silver enhancement combined with a second step of 10 nm gold particles, but

was not avoided by detection with the combination of 5 and 10 nm gold particles in the two steps.

Controls included omission of the primary antibody in the single immunolabelling, or omission of the first, the second or both primary antibodies in the double labelling experiments.

Analysis of vesicle size

We have used Lowicryl HM20 embedding since sections of this material can be immunolabelled with much higher efficiency than in Epon embedded material, although membranes of vesicles are not always visible as well as in Epon sections. The method of freeze substitution of nervous tissue and embedding in Lowicryl HM20 has been described previously[61] and can be seen as a compromise between the well known preservation of ultra structure (as in classical Epon embedding with osmium fixation) and the preservation of good antigenicity (as in cryo ultra microtomy). Osmium, which clearly stains membranes, is not used during the freeze substitution procedure. In principle, the contrast formed by interaction of the electron beam in the embedded tissue is not different for the two embedding procedures, but much weaker, when membranes are not stained with osmium. The contrast of membranes in the Lowicryl HM20 embedded tissue arises, for the largest part, from the counter staining procedure. For this reason, membranes, especially those surrounding small vesicles, are not always visible. The contour contrast of the vesicle, however, is usually easily recognized. Figure 1 shows a model of the interpretation of electron micrographs of the contrasted profiles of vesicles in

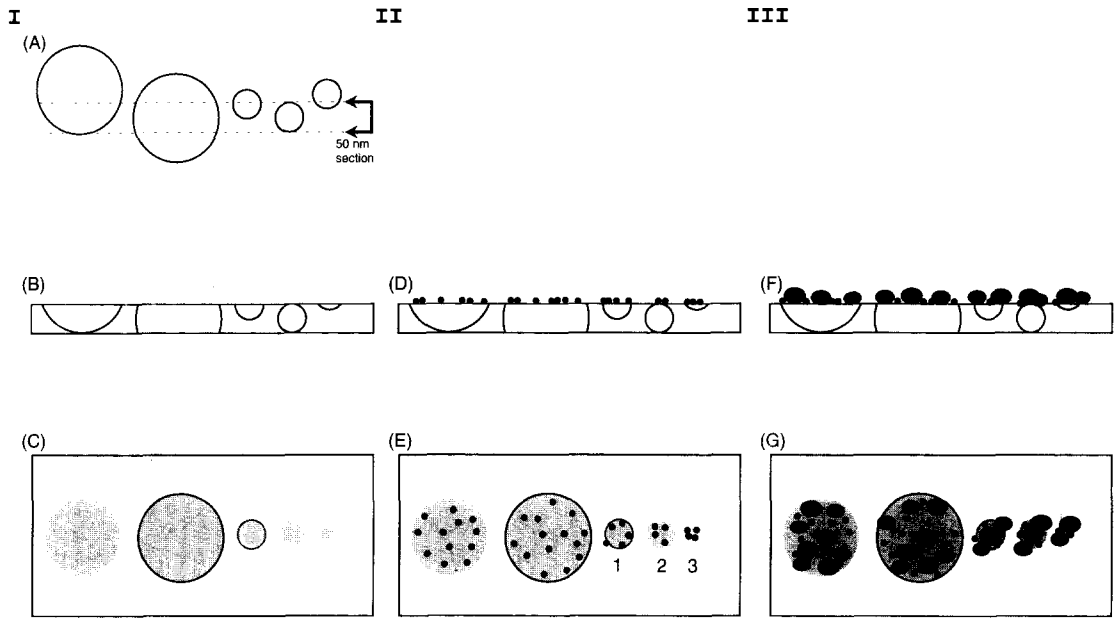

Fig. 1. Model for the interpretation as vesicles of contrasted semicircular profiles in electron micrographs of Lowicryl HM20 embedded material. (I) In unlabelled nerve sections. (A) Side view projection of unsectioned vesicles with diameters of 150 and 50 nm. The dotted line indicates where the vesicles will be sectioned by the ultracut. (B) Side view projection of a 50 nm section. Of the large 150 nm vesicles, only a part of the vesicle and membrane is contained within the section. The small 50 nm vesicles are also cut, but a larger part of the vesicle and even a complete vesicle can be within one section. Depending on how the electron beam hits the membrane of the vesicles and their cut parts, contrast of the vesicle and membrane will result. (C) The top view of the same section as in B with the resulting contrast. When the membrane of the vesicle is not cut perpendicular to the membrane but obliquely, the membrane will be hardly or not detectable by contrast with the surrounding. Cutting the membrane obliquely occurs very frequently when a small vesicle is sectioned, the membrane of a small vesicle will therefore be visualized in fewer occasions than larger vesicles. Vesicular profiles (=vesicles) are recognized by contrast to the surrounding. (II) In nerve sections with single labelling of a marker antigen that is present on both types of vesicles and is detected by 10 nm gold particles coated with the second antibody. (D) Side view projection of the section with 10 nm gold particle labelling (black dots) at the incubated top side of the section. (E) Top view of the same section as in D. Immunolabelling by 10 nm gold particles of large vesicles obscures the visibility of the vesicle somewhat. Labelling by 10 nm gold particles of small vesicles, however, may obscure the visibility of the vesicle depending on the plane of sectioning through the small vesicle. Based on the distinction of three main types of images, three types of immunolabelling of vesicles are recognized and described in Experimental Procedures (numbers 1, 2 and 3). (III) In nerve sections with double labelling of two different marker antigens by silver enhanced 1 nm gold particles and 10 nm gold particles. The antigens detected by the gold particles are present on both types of vesicles. (F) Side view projection of the section with 1 nm silver enhanced and 10 nm gold particle labelling at the top side of the nerve section. The silver enhanced gold particles usually vary in size and are irregular of shape. They are represented by two types of large oval black dots, the 10 nm gold particles are again visualized by the smaller round black dots. (G) Top view of the same section as in F. Depending on the labelling intensity and size of the 1 nm silver enhanced gold particles, the profile contrast and visibility of large vesicles may be obscured. Detection of the contour or contrast of small vesicles carrying 1 nm silver enhanced gold particles is a rare occasion. Therefore, small labelled vesicles are recognized by accumulation of the gold label revealing an antigen known to be present on such vesicles.

Lowicryl embedded material, with and without immunolabel. This model was used to distinguish the immunolabelled and unlabelled transport vesicles in the axoplasm of the Lowicryl HM20 embedded sciatic nerve pieces.

Nerve sections single labelled for B-50/GAP-43 and detected by 10 nm gold particles coated with second antibody were used for the analysis of the vesicle size. Recognition of vesicles thus labelled is easier than those immunolabelled with 1 nm silver enhanced gold particles, because as shown in Fig. 1, the last procedure usually obscures the vesicles. In order to be included in the analysis for the vesicle size, the immunolabelling had to be within a distance of 20 nm of the membrane of a vesicular profile[64] (Fig. 1E, type 1). In other cases, the membrane of the vesicular profile was not or incompletely visible, but the content of the vesicular profile was clearly distinct from the surrounding cytoplasm (Fig. 1E, type 2). Here we only included the profile in the analysis if four or more gold particles were attached with the profile. Gold particle clusters which obscured the vesicular profile (Fig. 1E, type 3) were not included in the analysis. In this way, a total of 164 labelled vesicular profiles from approximately five unmyelinated and five myelinated axons of the sciatic nerve pieces obtained from two adult rats were analysed by means of an automated system. For this analysis, a software application was developed for a PCVision Plus digitiser (Imaging Technology Inc.). This application digitises an image of the electron microscopic photo negative (magnification from 28,000 to 52,000×) placed under a CCD-camera. In these images labelled structures can be encircled by the user. The software calculates the area and diameter of each structure. These values are converted to real-world distances using a calibration factor. The number of gold particles in each structure was subsequently counted and each counted particle was marked.

The computerized method of determining the diameter of vesicles was verified by manually measuring vesicle size of 75 vesicular profiles in positives printed from the electron microscopic negatives which had been previously used in the computer analysis. This manual analysis showed the same size distribution as the analysis by computer.

RESULTS

Accumulation of anterogradely transported material

In order to characterize the types of transport vesicles to which B-50/GAP-43 is associated during anterograde axonal transport, we investigated portions of the regenerating sciatic nerve proximal to the nerve ligature. Immunofluorescence microscopy revealed that B-50/GAP-43 had accumulated, both, at the proximal and distal side of the ligation (results not shown). The accumulation is in agreement with previous findings of Tetzlaff *et al.*[54] and Li *et al.*[35]

We have restricted our ultrastructural study of the sciatic nerve, consisting of motor and sensory axons, to the anterograde axonal transport, interrupted at the proximal side of the ligature. For detailed analysis, electron micrographs of longitudinally sectioned myelinated and unmyelinated axons were taken from the proximal side of the ligature.

Examination of a region of a myelinated axon upstream from the ligature and closest to the cell body (approximately 50 μm proximal to the ligation), shows that in this region, as yet hardly any accumulation of intra-axonal organelles was apparent (Fig. 2A). A normal distribution of various types of vesicular profiles, mitochondria and also multivesicular bodies was present between the cytoskeletal network of microtubules and neurofilaments. Although many vesicular profiles were present, the morphological appearance of the axoplasm in this part was very similar to that of a myelinated axon in an intact nerve as described by Peters *et al.*[41]

Downstream, closer to the ligature (Fig. 2B), various types of membranous organelles, vesicular profiles and mitochondria started to accumulate, predominantly in the central portion of the axoplasm. Multivesicular bodies, which are considered to participate mainly in retrograde axonal transport[2,50] were only occasionally found in the axoplasm (Fig. 2B). As more organelles and particulate material accumulated, the cytoskeletal network appeared to be pushed to the peripheral axoplasm and gradually dissolved until small groups of neurofilaments were randomly oriented. This part of the axon seemed to be swollen (Fig. 2B). In other cases, however, the vesicular profiles started to accumulate at the periphery of the axon, while the cytoskeleton remained in the centre of the axon (not shown). This also resulted in a swelling of the axon and a gradual disappearance of the cytoskeletal network.

Even closer to the ligation, approximately 20 μm proximal to the ligation, the density of vesicular organelles was so high that the network of the cytoskeleton had completely disappeared (Fig. 2C). Numerous mitochondria and vesicular profiles of more or less uniform size had accumulated, but multivesicular bodies were virtually absent. Figure 2D shows, at larger magnification, that this part of the ligated axon contained clear and dark circular vesicular profiles surrounded by a recognizable membrane. Most of these vesicular profiles had a rather homogenous diameter of about 50 nm, in addition, there were also profiles present of larger diameter (ranging up to ±150 nm). Less frequent, membranous profiles were observed that had an elongated tubular structure. These, so called, tubulovesicular structures had a diameter of about 50 nm.

As shown in Fig. 3A, a similar accumulation of vesicular organelles and mitochondria occurred in regions, closest to the ligation, of unmyelinated axons. Visualization at higher magnification (Fig. 3B) demonstrates that, similar to the myelinated axon, an analogous diversity of vesicular profiles and tubulovesicular structures was present in unmyelinated axons.

B-50/growth-associated protein-43 immunolabelling

In order to exclude membranous organelles conveyed by the retrograde axonal transport, such as multivesicular bodies, and to focus on the anterogradely transported material, axon portions were sampled exclusively in regions proximal from the collection ligature which did not contain multivesicular bodies (from approximately 10 to 20 μm proximal

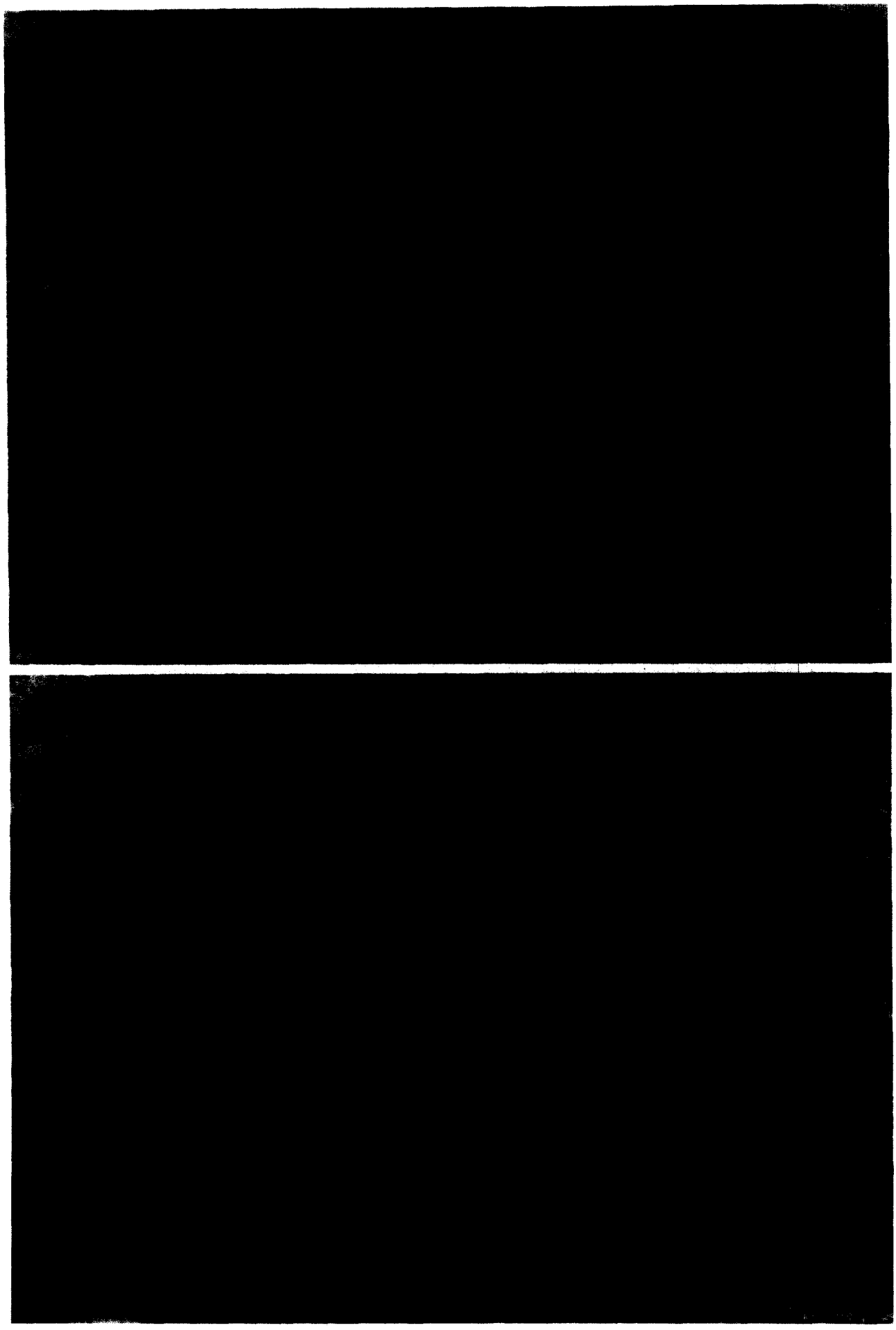

Fig. 2. (A, B)—*caption on page* 495

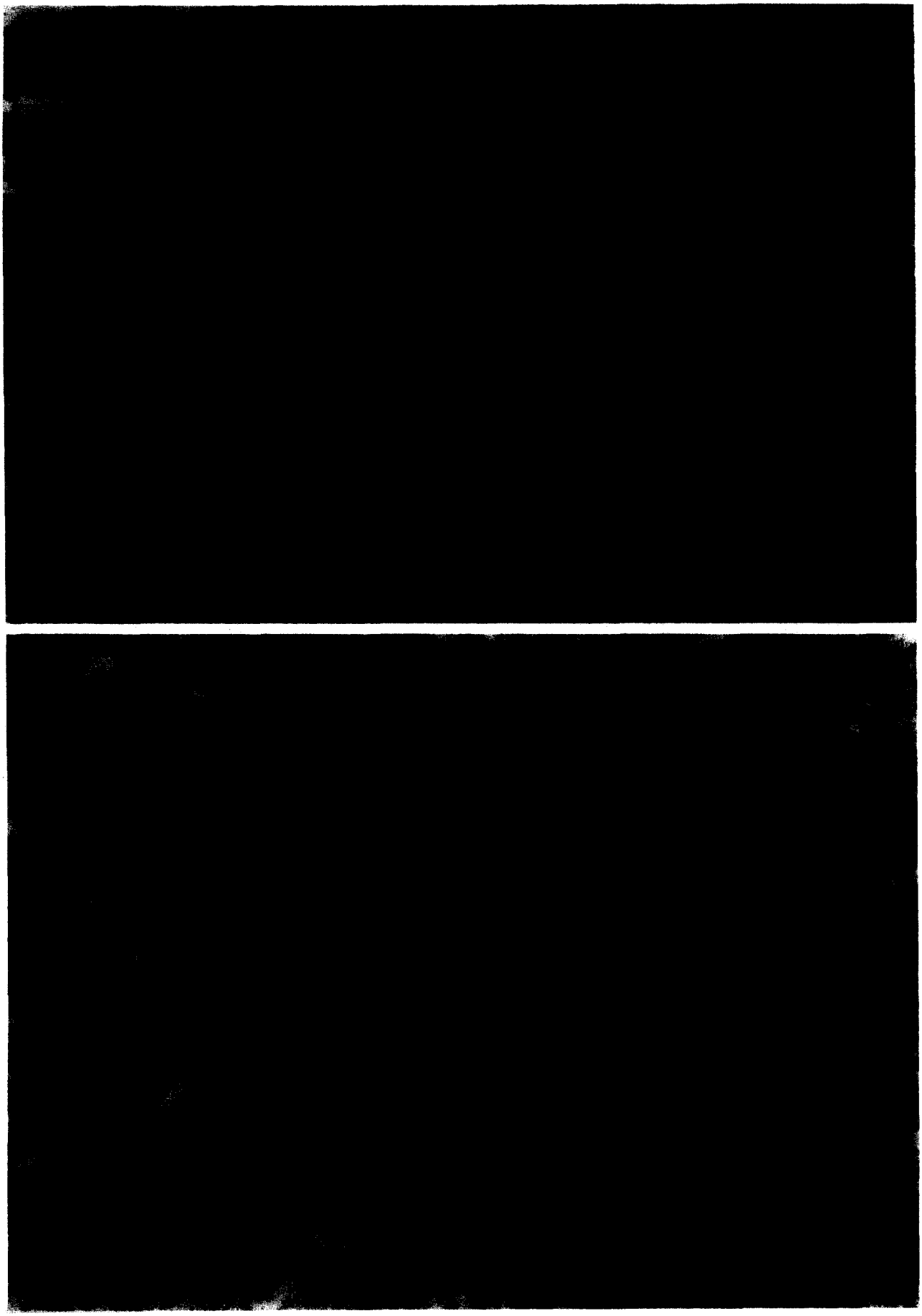

Fig. 2. (C, D)—*caption opposite.*

to the ligation; Figs 2C, D, 3A, B). In the accumulation of many types of vesicular profiles in the axoplasm of unmyelinated and myelinated axons, gold particles attached to the secondary antibody revealed the association of B-50/GAP-43 antibodies with certain vesicular profiles (Fig. 4). The gold particles were found on profiles containing a recognizable membrane (type 1), but also on circular profiles which were identified by contrast, but not by a boundary of membranes (type 2). From the total number of B-50/GAP-43-labelled profiles in the analysed electron micrographs, 44% were identified as having a clearly visible membrane (type 1) and 56% belonged to the type 2 vesicles. Gold particle clusters, probably detecting only a small part of a vesicle and thereby obscuring the visibility of the profile were also found (type 3), these clusters were not included in the vesicle analysis. Less than 10% of the accumulated vesicular profiles was identified as B-50/GAP-43 positive using 10 nm gold particles (approximately four B-50/GAP-43-labelled profiles/μm^2). The sensitivity of the detection of B-50/GAP-43-labelled profiles could be increased at least 2.5-fold by use of secondary antibodies attached to 1 nm gold particles and subsequently silver enhanced[18] (see Figs 7, 8). This silver enhancement procedure, however, obscured the visibility of the membranes of the vesicles, as described in Fig. 1.

Infrequent B-50/GAP-43 immunolabelling was detected in association of tubulovesicular profiles (Fig. 4B). An appreciable fraction of the gold particles, approximately 25% of the immunolabel, was not found in clusters and could not be located close to a particular identifiable structure. Gold particles which appeared not to be associated with organelles, may represent cytosolic or soluble B-50/GAP-43 or be associated with B-50/GAP-43 in structures which were not contrasted. Other organelles, such as mitochondria, were not immunolabelled. In agreement with our previous study[64] gold particles were also found in association with the axolemma of unmyelinated axons (Fig. 4C), but only rarely in myelinated axons.

Analysis of the diameter of B-50/growth-associated protein-43 immunolabelled vesicles

The distribution of the diameter of vesicular profiles immunolabelled for B-50/GAP-43 in myelinated and unmyelinated axons (78 and 86 vesicular profiles, respectively) did not show obvious differences; in both types of axons the immunolabelled profiles had a diameter ranging from 19 to 54 nm (Fig. 5). A vesicle diameter of about 19 nm reached the detection limit. Below 19 nm diameter, a vesicle could not be recognized. Only three immunolabelled profiles were found with a diameter exceeding 54 nm (63, 64 and 76 nm). Figure 5 shows the diagram for the various classes of diameter sizes measured from a total of 164 vesicular profiles. It is likely that the ultrathin sections were cut randomly through the volume of the vesicles, therefore we estimate that the maximum diameter is close to 47–54 nm, since vesicular profiles with a large diameter were rarely detected. Another way to calculate the diameter of vesicles from the measurements, is described by Hallet *et al.*[24] for freeze-fractured vesicles. It consists of multiplication of the mean size of the measured vesicles (35.1 ± 7.8) by $4/\pi$. This results in a vesicle diameter of 44.7 nm. To confirm that we were really dealing with vesicles and not with tubulovesicular structures in our embedded tissue, stereo micrographs were made and the images were placed so that the three-dimensional structure could be viewed. It showed that both the large and the small vesicle type, as presented in Fig. 1, were present and that the immunolabelling for B-50/GAP-43 was only found at the small vesicular profiles at the top of the section.

B-50/growth-associated protein-43 is partially co-localized with synaptophysin but not with calcitonin gene-related peptide

As stated above, the silver enhancement procedure could obscure the visibility of the vesicle membrane. For the co-localization of B-50/GAP-43 with either CGRP or synaptophysin, a double labelling procedure with silver enhancement was used. To demonstrate that our labelling for CGRP and synaptophysin was present only at vesicles, we also

Fig. 2. Accumulation of anterogradely transported material in the myelinated axon. Electron micrographs of a longitudinally sectioned myelinated axon from the proximal nerve region of the ligation, in which the upstream side is always at the left of the micrograph. In the region closest to the cell body (A), accumulation of intracellular structures was not present. The axon, which was surrounded by compacted myelin (M), contained some vesicular profiles (V), mitochondria (MT) and also multivesicular bodies (MB) inside the cytoskeletal network. Closer to the ligation (B), particulate material such as vesicular profiles and mitochondria started to accumulate. The cytoskeletal network of neurofilaments (NF) and microtubules was pushed laterally. Occasionally a multivesicular body was found. Closest to the ligation (C), the density of vesicular profiles and other material was so high that the network of the cytoskeleton was completely lost. Accumulation of mitochondria and a mass of vesicular profiles was found. A magnification of the marked region (D) shows that many of the membranous vesicular profiles appeared to have a uniform diameter (small vesicular profiles, SV). There were also some larger vesicular profiles (LV) present, and elongated membranous tubular structures (T). Scale bars: in A 500 nm for A–C, in D 200 nm.

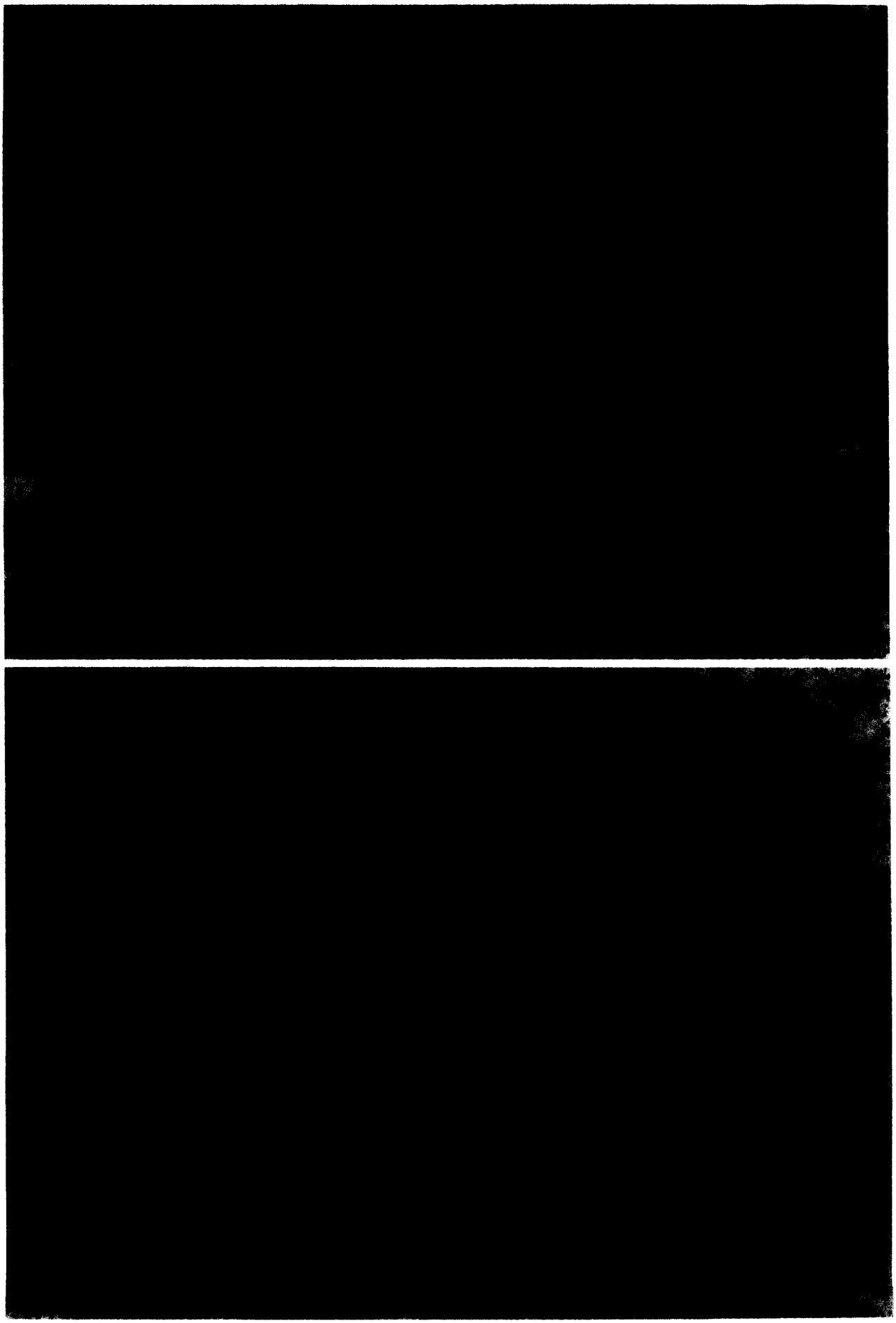

Fig. 3. (A, B)—*caption opposite.*

performed single labelling with 10 nm gold. It showed that immunolabel for synaptophysin and CGRP was almost exclusively present at vesicular profiles. Those carrying synaptophysin (Fig. 6A) were clearly smaller than the vesicular profiles labelled for CGRP (Fig. 6B). In the double labelling experiments we did not always find immunolabelling on membrane-bound vesicular profiles, but also on contrasted circular profiles that appeared to be vesicles (see Fig. 1) and sometimes only the presence of the vesicle markers, which were predominantly found in clusters, indicated the site of a vesicle. This disadvantage of the technique was of minor importance than the co-localization of the two antigens, since the vesicle markers synptophysin and CGRP were shown to be almost exclusively associated with membrane-bounded vesicular profiles in the single labelling procedure (see Fig. 6).

The procedure used for double labelling resulted in 10 nm gold particles that were seen as round and electron dense particles of uniform size. The 1 nm silver enhanced gold particles resulted in a little less electron dense particles that were irregular of shape and not uniform of size, ranging from approximately 10 to 40 nm. So electron dense particles of 10 nm could be distinguished by their shape and electron density.

In nerve sections taken from the proximal side of the nerve ligature, the double labelling procedure allowed detection of the localization of immunolabel for B-50/GAP-43 and synaptophysin (Fig. 7) to the same vesicle location. However, not all synaptophysin immunolabelled vesicle sites were also decorated by the immunolabel for B-50/GAP-43 and there were also B-50/GAP-43 decorated vesicle sites observed which were devoid of immunolabel for synaptophysin. Both, when antibodies to B-50/GAP-43 or synaptophysin were used as first primary antibody and detected by 1 nm gold particles, the immunolabelling density was much higher than when each antibody was applied in the second round as a second primary antibody and detected with 10 nm gold particles (see also below). No instances were observed in which the immunolabel of synaptophysin was associated with the axolemma.

Vesicular profiles carrying the immunolabel for CGRP had a diameter larger than the diameter of the B-50/GAP-43 immunolabelled profiles. With either of the two labelling procedures there was no co-localization between B-50/GAP-43 and CGRP (Fig. 8). Again detection with 1 nm gold particles showed a much higher labelling than detection with 10 nm gold particles (compare Fig. 8A and B). Notably, the CGRP immunolabel was not found in association with the axolemma.

Using the double labelling procedure CGRP and synaptophysin did not co-localize (not shown). In contrast to the antibodies to B-50/GAP-43, antibodies to these vesicle markers did not immunolabel tubular structures.

In order to check whether the detection of co-localization could be artefactual, control experiments were carried out. When the detection of the first primary antibody, using either one of the primary antibodies, was carried out by silver enhancement of 1 nm gold particles as usual, but then followed by the incubation step of the second primary antibody, without addition of this antibody, and further processing, as described, with the second immunolabel (the 10 nm gold particle-conjugate), there was no other immunolabel found than that of the silver enhanced gold particles of the first primary antibody (Fig. 9A–C). Omitting both primary antibodies gave no labelling at all (Fig. 9D).

DISCUSSION

Accumulation of anterograde transported material

In this study we have addressed the question by which type of vesicles B-50/GAP-43 may be transported anterogradely through axons of the rat sciatic nerve. In a former ultrastructural study,[64] we had observed that in the unobstructed regenerating sciatic nerve, vesicular organelles and vesicles carrying B-50/GAP-43 immunolabel occurred occasionally in the axoplasm of myelinated and unmyelinated axons. Here, we artificially induced accumulation of transported material by nerve ligation and studied this by immunoelectron microscopy. Ligation of nerves is a generally used method used to study axonal transport[13,21,26] and to accumulate transported organelles. As shown by our electron micrographs, ligation for 6 h of the regenerating sciatic nerve of the adult rat, resulted in accumulation of organelles and vesicular profiles of various sizes, tubular structures and mitochondria in both myelinated and unmyelinated axons at the proximal side of the ligature.

In the nerve sections taken from nerve pieces proximal to the ligation, a gradient in accumulating organelles was observed, with less dense accumulation at a greater distance from the ligation. This suggests that the accumulation was the consequence of anterograde transport of material. Moreover the accumulated material that was found proximal to the ligation was probably conveyed by the fast

Fig. 3. Accumulation of anterogradely transported material in the unmyelinated axon. In the proximal nerve region closest to the ligature (A), several unmyelinated axons separated by their darkly contrasted plasma membrane (PM) contained an accumulation of mitochondria (MT), small (SV) and large (LV) vesicular profiles, and the so-called tubulovesicular structures (T; in B). Scale bars: in A 500 nm and in B 200 nm.

component of the anterograde transport since accumulation of calmodulin (which is transported by the slow component[8]) was not found (not shown). Nerve portions distant from the ligature, with little accumulation, containing multivesicular bodies, were not examined in detail, since retrograde transport in these parts could have occurred as well.

Our results, particularly, the ultrastructure of the accumulating mass of tubulovesicular membranous organelles in myelinated axons may be compared with ultrastructural studies reported earlier. Hirokawa *et al.*[26] investigated the association of kinesin, the microtubule-activated ATPase, with vesicles in the ligated saphenous nerve of the mouse, using a different immunoelectron microscopic procedure, namely immuno cryo ultra microtomy. The kinesin-labelled carriers were revealed as vesicular profiles accumulating proximal to the ligation.

Though less frequently, we observed the accumulation of tubulovesicular membranous profiles. These results may be compared with the findings previously reported by Tsukita and Ishikawa.[55] They had used local cooling of the mouse saphenous nerves to interrupt axonal transport and found that

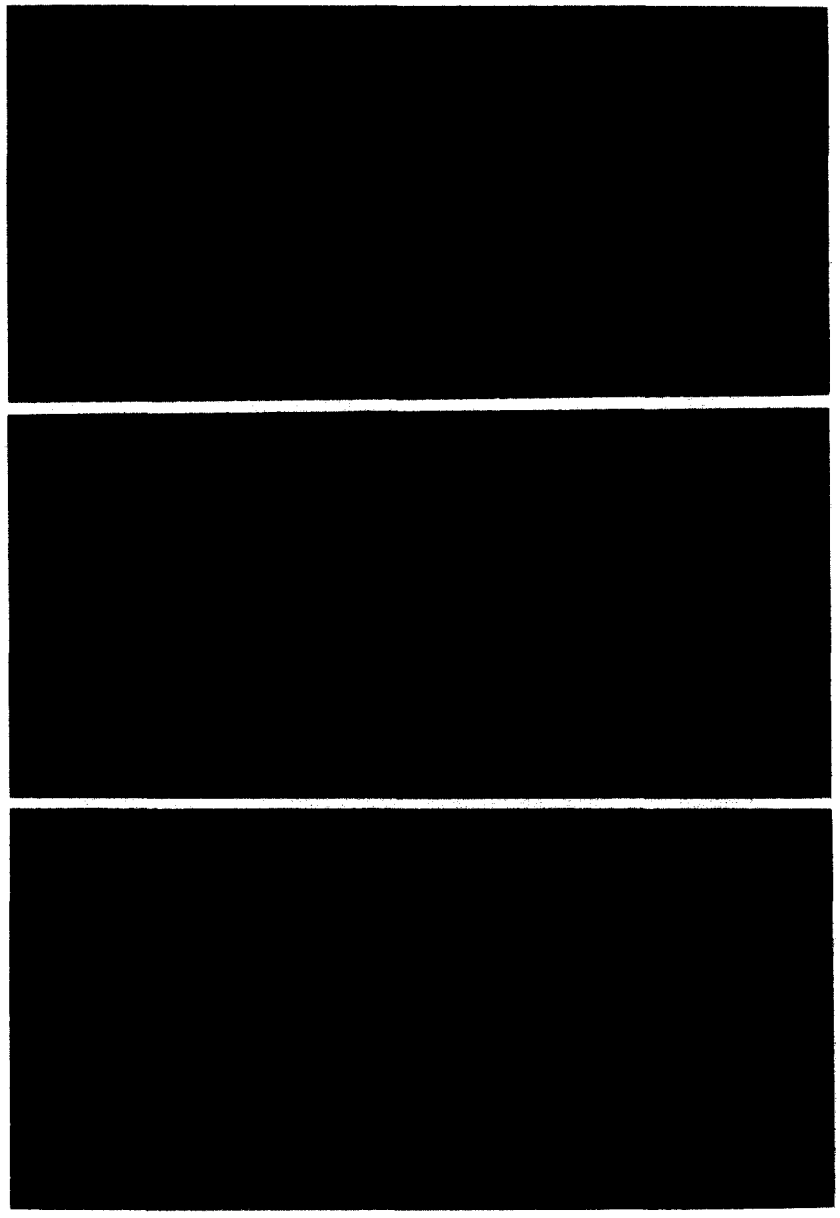

Fig. 4. B-50/GAP-43 is associated with vesicular structures. Electron micrographs showing B-50/GAP-43 immunolabelling at vesicular and tubular membranous structures in the axoplasm. A shows vesicular profiles of the types 1 and 2 (see Experimental Procedures). B shows a type 2 and a type 3 vesicular profile, tubulovesicular structures (T), decorated with gold particles detecting B-50/GAP-43, were rarely found. (C) In unmyelinated axons besides vesicular labelling, labelling at the plasma membrane (arrows) was also detected. Scale bar: 100 nm.

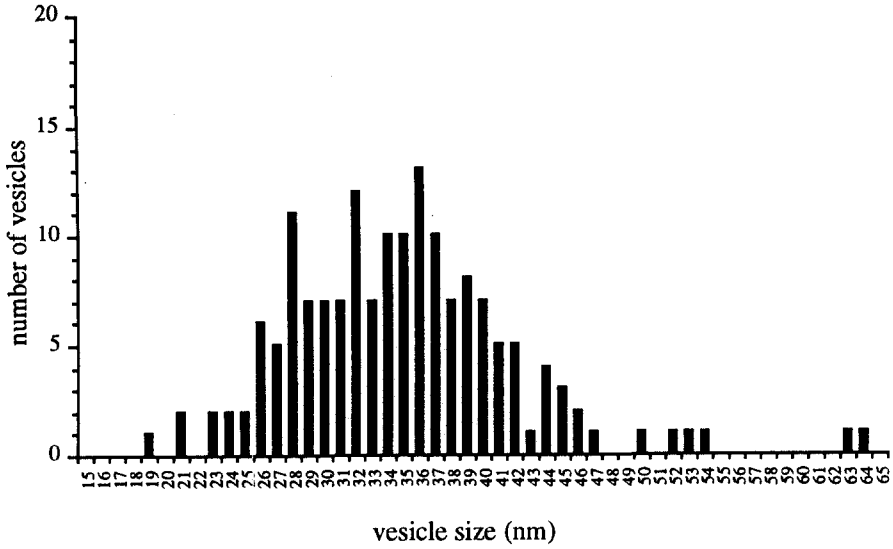

Fig. 5. B-50/GAP-43 is associated with vesicles with a diameter of 50 nm. The distribution of the diameter of B-50/GAP-43 immunolabelled vesicular profiles shows that the largest diameter of a B-50/GAP-43 immunolabelled profile is around 50 nm. The number of profiles of a particular size (y-axis) is plotted against the diameter of the profile (x-axis).

tubulovesicular membranous structures increased in amount just proximal to the cooled site, at which site radioactively labelled, anterogradely transported proteins were shown to accumulate. This suggested that the accumulated organelles were the carriers of the labelled proteins. The accumulated membranous structures displayed a relative uniform diameter of 50–80 nm and some of them seemed to be continuous with the axonal SER.[55]

It has been proposed that the tubulovesicular membranous structures may form a continuous network from the cell body to the nerve terminals,[2,3] forming an intracellular alternative transport pathway to the generally accepted model of targeted transport by carrier vesicles.[44,51] However, it may be that both the vesicular and the tubulovesicular transport route may exist in the same cell; such a conclusion was reached from electron microscopic studies on serial sections. Since in single sections, a sectioned vesicle can not be distinguished from a cross-sectioned tubule of the same diameter, it is possible that the many round vesicular structures of ± 50 nm which we found originated from tubular structures. We verified this possibility with stereo images and saw mainly vesicular profiles sectioned at different planes. Therefore, we consider that the accumulation of the vesicular profiles in the sciatic nerve is the result of anterograde transport as mediated by vesicular carriers.

B-50/growth-associated protein-43 is anterogradely transported with 50 nm vesicles

In the last decade, several reports have documented that B-50/GAP-43 is transported anterogradely by

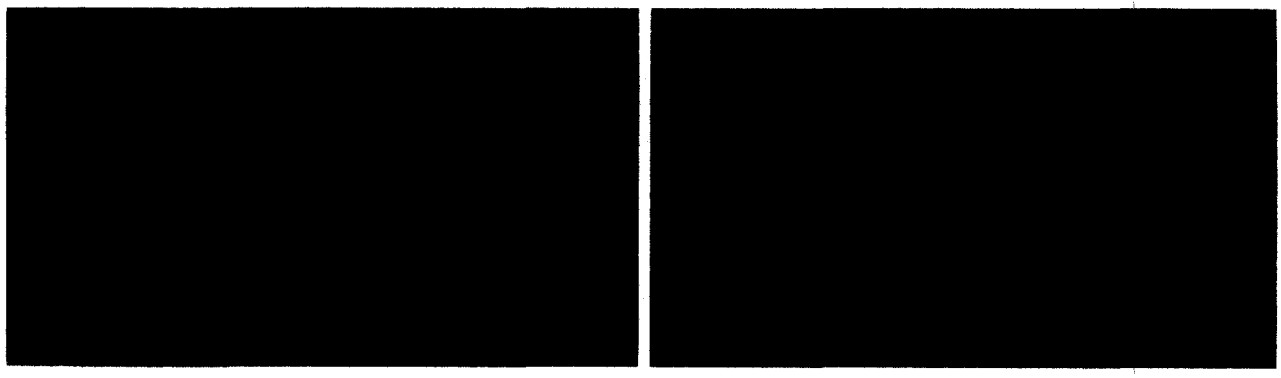

Fig. 6. Synaptophysin and CGRP are associated with vesicles. Synaptophysin and CGRP, which we used as vesicle markers, were found at vesicular profiles, as was detected by the 10 nm gold particles. (A) Shows synaptophysin immunogold labelling at three small vesicular profiles. (B) shows CGRP immunogold labelling at two large vesicular profiles. The profiles labelling for CGRP are clearly larger than those labelling for synaptophysin. Scale bar: 100 nm.

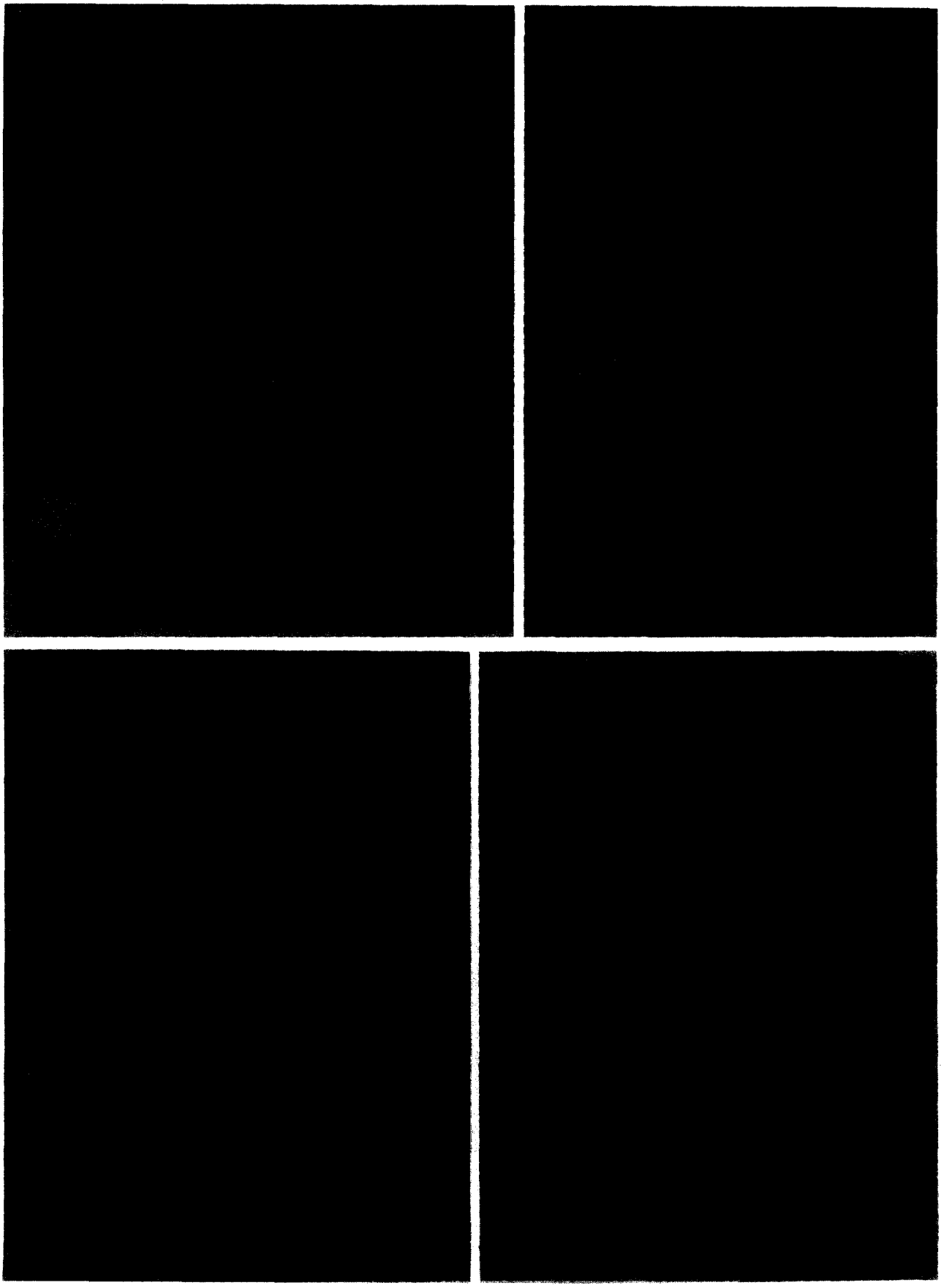

Fig. 7. (A–D)—*caption opposite.*

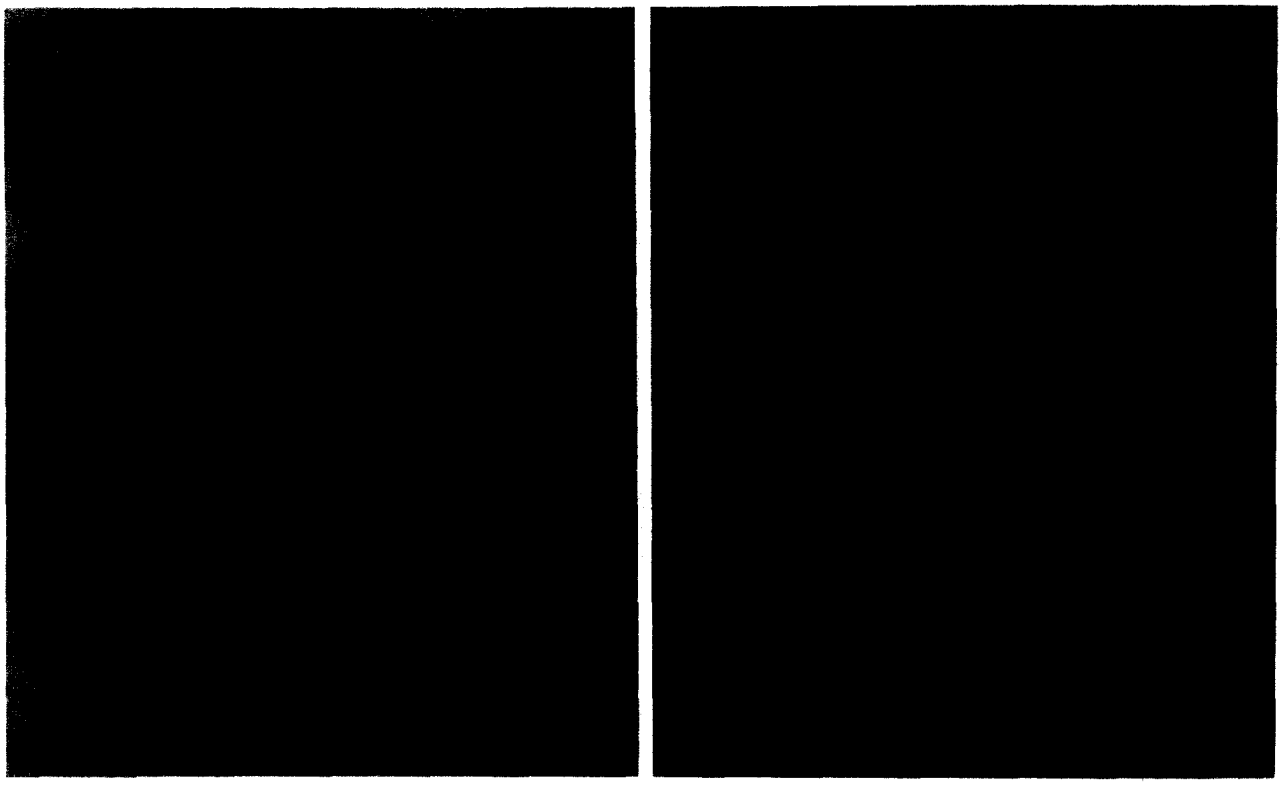

Fig. 8. B-50/GAP-43 does not co-localize with CGRP. B-50/GAP-43 does not show co-localization with the large dense core vesicle marker CGRP as demonstrated by both immuno double labelling sequences. (A) CGRP was detected by the 1 nm silver enhanced gold particles and B-50/GAP-43 by the small 10 nm gold particles. (B) Switching the primary antibodies did not change the immunolabelling pattern (CGRP small 10 nm gold particles and B-50/GAP-43 1 nm silver enhanced gold particles, ranging from 10 to 40 nm). The densities of immunolabelling were, however, clearly influenced by the switching of the secondary antibodies. The density of B-50/GAP-43 immunolabel was clearly increased by switching the detection from 10 nm gold particles (A) to detection by 1 nm gold particles and subsequent silver enhancement (B), while the immunolabel for CGRP clearly decreased from A to B. Scale bar: 100 nm.

fast axonal transport,[5,6,27,31,46,48,49] in association with membranous material.[47] Our study tries to uncover the carrier of this transport in the rat sciatic nerve, at the ultrastructural level. Amidst various accumulated organelles at the proximal side of the sciatic nerve ligature, gold particles, revealing B-50/GAP-43, were shown to be located at vesicular profiles and, rarely, at tubulovesicular membrane structures. Measurements of the diameter of the vesicle profiles, decorated by B-50/GAP-43 immunolabel, resulted in an extrapolated value of 47–54 nm for the average diameter of these vesicles. This vesicle diameter corresponds very well with the small 50 nm anterograde transport vesicles found in various other ultrastructural studies.[19,50,55] Since clearly not all the small vesicular profiles were labelled for B-50/GAP-43 and almost no labelled profiles larger than 54 nm were found, B-50/GAP-43 was probably transported by a subgroup (or type) of anterograde transport vesicles.

In an ultrastructural study of developing hippocampal neurons *in vitro*, Van Lookeren Campagne *et al.*[58,59] demonstrated that B-50/GAP-43 immunolabelling was present at clear vesicles, detected in the trans region of the Golgi apparatus, adjoining microtubules in the cell body, in neurites and growth

Fig. 7. B-50/GAP-43 co-localizes partially with synaptophysin. Electron micrographs showing immunogold double labelling of B-50/GAP-43 and the vesicle marker synaptophysin. (A, B) B-50/GAP-43 (small 10 nm gold particles) was found in close proximity to a cluster of synaptophysin immunolabel (large 1 nm silver enhanced gold particles), indicating the presence of B-50/GAP-43 and synaptophysin on the same vesicle (large arrows). Not all synaptophysin immunolabel clusters also contained B-50/GAP-43 and vice versa, as shown by the small arrows pointing to clusters solely labelled for B-50/GAP-43. (C, D) Switching the sequence of primary antibody labelling showed an increase in labelling for B-50/GAP-43 and a decrease for synaptophysin. This finding did not alter the types of immunolabelled clusters that were found. This labelling also showed clusters which contained label both for B-50/GAP-43 (large 1 nm silver enhanced gold particles) and synaptophysin (small 10 nm gold particles; large arrows), and clusters containing only label for one of the proteins. Scale bar: 100 nm.

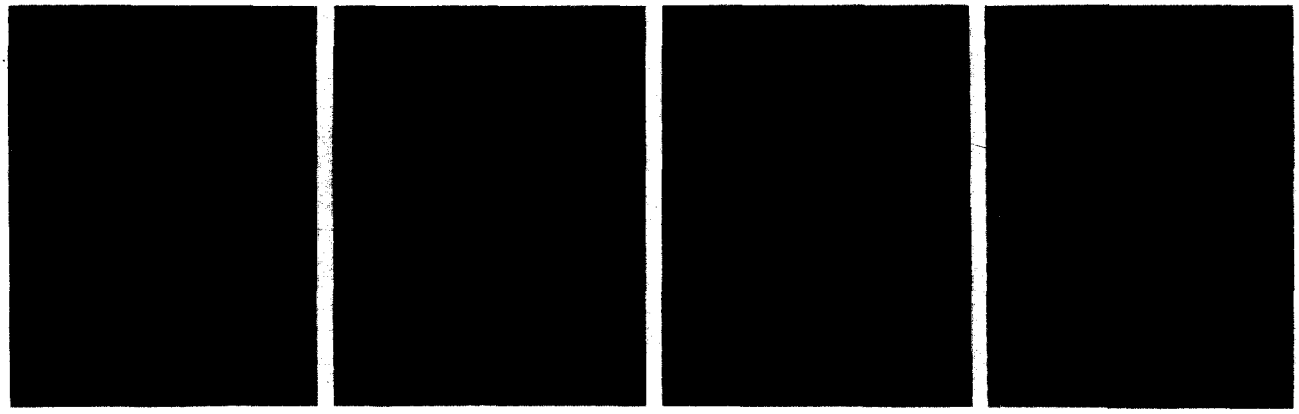

Fig. 9. The immunogold double labelling procedure does not show cross-reactivity. Electron micrographs showing specificity of the double labelling experiments. Antibodies to B-50/GAP-43 (A), synaptophysin (B), and CGRP (C) were detected by silver enhanced 1 nm gold particles. No second primary antibody was added and after detection by 10 nm gold particles, only silver enhanced gold particles were found. When both primary antibodies (D) were omitted no labelling was found. Scale bar: 100 nm.

cones of the hippocampal neurons. These vesicles were visualized as electron lucent membrane-bounded structures with an average diameter of 100 nm. The B-50/GAP-43 decorated clear vesicles in hippocampal neurons were detected all along the constitutive axonal transport pathway, which is known to involve intact microtubules and carrier-associated motor proteins.[7] This study did not directly address the issue of the transport direction of the immunolabelled vesicles and the pathways. It was suggested that the vesicles were translocated mainly along the anterograde route. Here we limited our analysis to the anterograde transport route in the rat sciatic nerve, but comparison of these studies suggests that different types of neurons may use various kinds of transport carriers.

Various types of transport vesicles move rapidly anterogradely in the regenerating rat sciatic nerve

A multitude of vesicular profiles was seen to accumulate proximal to the nerve ligation; of these profiles a fraction was immunolabelled for B-50/GAP-43 and the vesicle marker proteins. The nature of the B-50/GAP-43 carriers in the sciatic nerve was characterized, partially by double labelling experiments, using synaptophysin, as a marker for STV. The STV are vesicular structures which have a diameter of approximately 50 nm and consist of various types of vesicles of different protein composition involved in the targeting to either the axolemma or the axon terminal.[38] STV containing synaptophysin are thought to be routed specifically to the axon terminal.[2,38] STV are capable of fusion with the plasma membrane and in the axon terminal can be recycled by endocytosis to form small synaptic vesicles.[32] In PC12 cells, synaptophysin is transported out of the cell body by the constitutive vesicle transport pathway, then found transiently at the cell surface, next in an intracellular endosome-like compartment and finally in small synaptic vesicles.[42] We demonstrate that a fraction of transported B-50/GAP-43 immunolabel was conveyed on vesicles which also contained synaptophysin immunolabel. In addition, it is shown that there was also a population of vesicles immunolabelled solely for B-50/GAP-43 and another population with immunolabel only for synaptophysin. Therefore, it is possible that in our study, at least three subtypes of small transport vesicles have been distinguished by the immunolabels. Since by the post-embedding immunolabelling procedure, the specific antigens were very likely not revealed totally, it can not be excluded that the subtypes carried one of the antigens in an inaccessible place and, therefore the distinction in different subtypes of vesicles may be apparent. Based on the results of the double immunolabelling experiments, which when carried out in reverse order, also showed three types of vesicles, we prefer the possibility of various subtypes.

B-50/GAP-43 is also present in peripheral axons that contain CGRP as shown by light microscopy.[9,43] This neuropeptide, which is present in spinal cord motor neurons and widely distributed in the peripheral nervous system, was found to be located on spherical LDCV[23] with a diameter of approximately 100 nm.[50] Our results reveal CGRP in large vesicular profiles which were not associated with B-50/GAP-43 immunoreactivity. This suggests that B-50/GAP-43 is not co-transported with CGRP in the axoplasm of the sciatic nerve. Since neuropeptides are transported via the regulated exocytotic pathway of the LDCV,[16] it is likely that B-50/GAP-43 is not conveyed by carriers of this pathway in the sciatic nerve.

Our ultrastructural results are in fair agreement with other light microscopic studies. Recently Li *et al.*[35] used immunofluorescence light and confocal

laser microscopy to study the distribution of B-50/GAP-43 with markers of vesicles during axonal transport in the sciatic nerve of adult rat. To observe the accumulation of the transported proteins they placed two crushes within 1–2 mm distance. They found that the amounts of B-50/GAP-43-like immunoreactivity increased both proximal and distal to the crush site in the first day after crushing the sciatic nerve. Transported synaptophysin behaved similarly. Double immunolabelling of the sciatic nerve axons for both antigens showed that B-50/GAP-43 and synaptophysin were partially co-localized and transported in the same axon, but these proteins appeared not to be stored in the same intra-axonal organelles. Li *et al.*[35] concluded that B-50/GAP-43 is bidirectional transported through the normal sciatic nerve.

In another study[34] by confocal laser scanning microscopy, the distribution of B-50/GAP-43, synaptophysin and CGRP during development of rat skeletal muscles was reported. Li *et al.*[34] found that during development and in adulthood B-50/GAP-43 immunoreactivity was strong in small and large granules of perivascular nerve terminals. In a few thin sensory axons large granules were labelled by the B-50/GAP-43 antibodies, but there was no co-localization between B-50/GAP-43 and CGRP. These confocal light microscopic studies have revealed the subcellular compartment in which the studied antigens are located, but they do not reach sufficient resolution to demonstrate subcompartmental localization, such as association with particular organelles or carriers.

B-50/growth-associated protein-43 may be transported to the axon terminal and the axolemma in two different types of constitutive transport vesicles

It is attractive to speculate about the function of the two detected populations of B-50/GAP-43 immunolabelled vesicles, namely those containing, in addition, synaptophysin ($p38^+$/B-50) and those being negative for synaptophysin ($p38^-$/B-50). Local incorporation of proteins into the axolemma, probably by means of vesicle fusion, has been suggested.[22] In a previous ultrastructural study,[64] we discovered that during axonal regeneration of the sciatic nerve in the adult rat, the proximal axolemma of unmyelinated axons was enriched in B-50/GAP-43 in comparison to the intact unmyelinated axon. In line with this finding, it could be that B-50/GAP-43 carrying vesicles locally fuse with unmyelinated axolemma and attach B-50/GAP-43 during the translocation. Since no instance was found of synaptophysin (p38) labelling on the axolemma, the $p38^-$/B-50 vesicles could be targeted to the axolemma, whereas the $p38^+$/B-50 vesicles could continue their travel to the growth cone and nerve terminal.

Future studies, in which subcellular fractions are made from ligated nerve and vesicles are isolated, are of great interest for further characterization of B-50/GAP-43 carrying vesicles.

Acknowledgements—The authors would like to thank Jan Brakkee and Marlou Josephy for their skilful assistance in the surgical procedures and Theo van der Krift in assistance with designing the model of Fig. 1.

REFERENCES

1. Aigner L. and Caroni P. (1995) Absence of persistent spreading, branching, and adhesion in GAP-43-depleted growth cones. *J. Cell Biol.* **128,** 647–660.
2. Annaert W. G., Quatacker J., Llona I. and De Potter W. P. (1994) Differences in the distribution of cytochrome b_{561} and synaptophysin in dog splenic nerve: a biochemical and immunocytochemical study. *J. Neurochem.* **62,** 265–274.
3. Ayala J. S. (1994) Transport and internal organization of membranes: vesicles, membrane networks and GTP-binding proteins. *J. Cell Sci.* **107,** 753–763.
4. Benowitz L. I., Apostolides P. J., Perrone-Bizzozero N. I., Finklestein S. P. and Zwiers H. (1988) Anatomical distribution of the growth-associated proteins GAP-43/B-50 in the adult rat brain. *J. Neurosci.* **8,** 339–352.
5. Benowitz L. I. and Lewis E. R. (1983) Increased transport of 44,000 to 49,000 dalton acidic proteins during regeneration of the goldfish optic nerve: a two-dimensional gel analysis. *J. Neurosci.* **3,** 2153–2163.
6. Bisby M. A. (1988) Dependence of GAP43 (B50, F1) transport on axonal regeneration in rat dorsal root ganglion neurons. *Brain Res.* **458,** 157–161.
7. Brady S. (1985) A novel brain ATPase with properties expected for the fast axonal transport motor. *Nature* **317,** 73–75.
8. Brady S. T., Tytell M., Heriot K. and Lasek R. J. (1981) Axonal transport of calmodulin: a physiological approach to identification of long-term associations between proteins. *J. Cell Biol.* **89,** 607–614.
9. Buma P., Verschuren C., Versleyen D., van der Kraan P. and Oestreicher A. B. (1992) Calcitonin gene-related peptide, substance P and GAP-43/B-50 immunoreactivity in the normal and arthrotic knee joint of the mouse. *Histochemistry* **98,** 327–339.
10. Chong M. S., Fitzgerald M., Winter J., Hutsai M., Emson P. C., Wiese U. and Woolf C. J. (1992) GAP-43 messenger RNA in rat spinal cord and dorsal root ganglia neurons—developmental changes and re-expression following peripheral nerve injury. *Eur. J. Neurosci.* **4,** 883–895.
11. Curtis R., Stewart H. J. S., Hall S. M., Wilkin G. P., Mirsky R. and Jessen K. R. (1992) GAP-43 is expressed by nonmyelin-forming Schwann cells of the peripheral nervous system. *J. Cell Biol.* **116,** 1455–1464.
12. Dahlström A. (1983) Presence, metabolism and axonal transport of transmitters in peripheral mammalian axons. In *Handbook of Neurochemistry* (ed. Lajtha A.), pp. 405–442. Plenum, New York.
13. Dahlström A. and Booj S. (1988) Rapid axonal transport as a chromatographic process: the use of immunocytochemistry of ligated nerves to investigate the biochemistry of anterogradely versus retrogradely transported organelles. *Cell Motil. Cytoskeleton* **10,** 309–320.

14. Dani J. W., Armstrong D. M. and Benowitz L. I. (1991) Mapping the development of the rat brain by GAP-43 immunocytochemistry. *Neuroscience* **40,** 277–287.
15. Danscher G. (1981) Localization of gold in biological tissue: a photochemical method for light and electronmicroscopy. *Histochemistry* **71,** 81–88.
16. De Camilli P. and Jahn R. (1990) Pathways to regulated exocytosis in neurons. *A. Rev. Physiol.* **52,** 625–645.
17. De Koning P., Brakkee J. and Gispen W. H. (1986) Methods for producing a reproducible crush in the sciatic and tibial nerve of the rat and rapid and precise testing of return of sensory function. *J. neurol. Sci.* **74,** 237–246.
18. Dulhunty A. F., Junankar P. R. and Stanhope C. (1993) Immunogold labeling of calcium ATPase in sarcoplasmic reticulum of skeletal muscle—use of 1-nm, 5-nm and 10-nm gold. *J. Histochem. Cytochem.* **41,** 1459–1466.
19. Fahim M. A., Lasek R. J., Brady S. T. and Hodge A. J. (1985) AVEC-DIC and electron microscopic analysis of axonally transported particles in cold-blocked squid giant axons. *J. Neurocytol.* **14,** 689–704.
20. Gispen W. H., Nielander H. B., De Graan P. N. E., Oestreicher A. B., Schrama L. H. and Schotman P. (1991) Role of the growth-associated protein B-50/GAP-43 in neuronal plasticity. *Molec. Neurobiol.* **5,** 61–85.
21. Grafstein B. and Forman D. S. (1980) Intracellular transport in neurons. *Physiol. Rev.* **60,** 1167–1283.
22. Griffin J. W., Price D. L., Drachman D. B. and Morris J. (1981) Incorporation of axonally transported glycoproteins into axolemma during nerve regeneration. *J. Cell Biol.* **88,** 205–214.
23. Gulbekian S., Merighi A., Wharton J., Varndell I. M. and Polak J. M. (1986) Ultrastructural evidence for the coexistence of calcitonin gene-related peptide and substance P in secretory vesicles of peripheral nerves of the guinea pig. *J. Neurocytol.* **15,** 535–542.
24. Hallet F. R., Nickel B., Samuels C. and Krygsman P. H. (1991) Determination of vesicle size distributions by freeze-fracture electron microscopy. *J. Electron Microsc. Tech.* **17,** 459–466.
25. Hens J. J., De Wit M., Boomsma F., Mercken M., Oestreicher A. B., Gispen W. H. and De Graan P. N. (1995) N-terminal-specific anti-B-50 (GAP-43) antibodies inhibit (Ca(2+)-induced noradrenaline release, B-50 phosphorylation and dephosphorylation, and calmodulin binding. *J. Neurochem.* **64,** 1127–1136.
26. Hirokawa N., Sato-Yoshitake R., Kobayashi N., Pfister K. K. and Bloom G. S. (1991) Kinesin associates with anterogradely transported membranous organelles *in vivo*. *J. Cell Biol.* **114,** 295–302.
27. Hoffman P. N. (1989) Expression of GAP-43, a rapidly transported growth-associated protein, and class II beta-tubulin, a slowly transported cytoskeletal protein, are coordinated in regenerating neurons. *J. Neurosci.* **9,** 893–897.
28. Jacobsen R., Virag I. and Skene J. H. P. (1986) A protein associated with axon growth, GAP-43, is widely distributed and developmentally regulated in rat CNS. *J. Neurosci.* **6,** 1843–1855.
29. Jahn R., Schliebler W., Ouimet C. and Greengard P. (1985) A 38,000 dalton membrane protein (p38) present in synaptic vesicles. *Proc. natn. Acad. Sci. U.S.A.* **82,** 4137–4141.
30. Jahn R. and Südhof T. C. (1994) Synaptic vesicles and exocytosis. *A. Rev. Neurosci.* **17,** 219–246.
31. Kalil K. and Skene J. H. P. (1986) Elevated synthesis of an axonally transported protein correlates with axon outgrowth in normal and injured pyramidal tracts. *J. Neurosci.* **6,** 2563–2570.
32. Kelly R. B. and Grote E. (1993) Protein targeting in the neuron. *A. Rev. Neurosci.* **16,** 95–127.
33. Kruger L., Bendotti C., Rivolta R. and Samanin R. (1993) Distribution of GAP-43 mRNA in the adult rat brain. *J. comp. Neurol.* **333,** 417–434.
34. Li J.-Y. and Dahlström A. (1993) Distribution of GAP-43 in relation to CGRP and synaptic vesicle markers in rat skeletal muscles during development. *Devl Brain Res.* **74,** 269–282.
35. Li J.-Y., Kling-Petersen A. and Dahlström A. (1993) GAP 43-like immunoreactivity in normal adult rat sciatic nerve, spinal cord, and motoneurons: axonal transport and effect of spinal cord transection. *Neuroscience* **57,** 759–776.
36. Liu Y. C., Fisher D. A. and Storm D. R. (1993) Analysis of the palmitoylation and membrane targeting domain of neuromodulin (GAP-43) by site-specific mutagenesis. *Biochemistry* **32,** 10,714–10,719.
37. McGuire C. B., Snipes G. J. and Norden J. (1988) Light-microscopic immunolocalization of the growth- and plasticity-associated protein GAP-43 in the developing brain. *Devl Brain Res.* **41,** 277–291.
38. Morin P. J., Liu N., Johnson R. J., Leeman S. E. and Fine R. E. (1991) Isolation and characterization of rapid transport vesicle subtypes from rabbit optic nerve. *J. Neurochem.* **56,** 415–427.
39. Ochs S. (1974) Systems of material transport in nerve fibers (axoplasmic transport) related to nerve function and trophic control. *Ann. N.Y. Acad. Sci.* **228,** 202–223.
40. Oestreicher A. B., Van Dongen C. J., Zwiers H. and Gispen W. H. (1983) Affinity-purified anti-B-50 protein antibody: interference with the function of the phosphoprotein B-50 in synaptic plasma membranes. *J. Neurochem.* **41,** 331–340.
41. Peters A., Palay S. L. and De Webster H. F. (1976) *The Fine Structure of the Nervous System: the Neurons and Supporting Cells.* Saunders, Toronto.
42. Régnier-Vigouroux A., Tooze S. A. and Huttner W. B. (1991) Newly synthesized synaptophysin is transported to synaptic-like microvesicles via constitutive secretory vesicles and the plasma membrane. *Eur. molec. Biol. Org. J.* **10,** 3589–3601.
43. Risling M., Dalsgaard C.-J., Frisén J., Sjogren A. M. and Fried K. (1994) Substance P-, Calcitonin Gene-Related Peptide, Growth-Associated Protein-43, and Neurotrophin Receptor-like immunoreactivity associated with unmyelinated axons in Feline ventral roots and pia mater. *J. comp. Neurol.* **339,** 365–386.
44. Rothman J. E. and Orci L. (1992) Molecular dissection of the secretory pathway. *Nature* **355,** 409–415.
45. Scherer S. S., Xu Y.-T., Roling D., Wrabetz L., Feltri M. L. and Kamholz J. (1994) Expression of growth-associated protein-43 kD in Schwann cells is regulated by axon-Schwann cell interactions and cAMP. *J. Neurosci. Res.* **38,** 575–589.
46. Skene J. H. P. (1989) Axonal growth-associated proteins. *A. Rev. Neurosci.* **12,** 127–156.
47. Skene J. H. P. and Virag I. (1989) Posttranslational membrane attachment and dynamic fatty acylation of a neural growth cone protein, GAP-43. *J. Cell Biol.* **108,** 613–624.
48. Skene J. H. P. and Willard M. B. (1981) Changes in axonally transported proteins during axon regeneration in toad retinal ganglion cells. *J. Cell Biol.* **89,** 86–95.
49. Skene J. H. P. and Willard M. B. (1981) Axonally transported proteins associated with axon growth in rabbit central and peripheral nervous systems. *J. Cell Biol.* **89,** 96–103.
50. Smith R. S. (1980) The short term accumulation of axonally transported organelles in the region of localized lesions of single myelinated axons. *J. Neurocytol.* **9,** 39–65.

51. Söllner T., Whitehart S. W., Brunner M., Erdjumentbromage H., Geromanos S., Tempst P. and Rothman J. E. (1993) SNAP receptors implicated in vesicle targeting and fusion. *Nature* **362,** 318–324.
52. Strittmatter S. M., Fankhauser C., Huang P. L., Mashimo H. and Fishman M. C. (1995) Neuronal pathfinding is abnormal in mice lacking the neuronal growth cone protein GAP-43. *Cell* **80,** 445–452.
53. Strittmatter S. M., Vartanian T. and Fishman M. C. (1992) GAP-43 as a plasticity protein in neuronal form and repair. *J. Neurobiol.* **23,** 507–520.
54. Tetzlaff W., Zwiers H., Lederis K., Cassar L. and Bisby M. A. (1989) Axonal transport and localization of B-50/GAP-43-like immunoreactivity in regenerating sciatic and facial nerves of the rat. *J. Neurosci.* **9,** 1303–1313.
55. Tsukita S. and Ishikawa H. (1980) The movement of membranous organelles in axons: electron microscopic identification of anterogradely and retrogradely transported organelles. *J. Cell Biol.* **84,** 513–530.
56. Ulenkate H. J. L. M., Verhaagen J., Plantinga L. C., Mercken M., Veldman H., Jennekens F. G. I., Gispen W. H. and Oestreicher A. B. (1993) Upregulation of B-50/GAP-43 in Schwann cells at denervated motor endplates and in motoneurons after rat facial nerve crush. *Restor. Neurol. Neurosci.* **6,** 35–47.
57. Van der Zee C. E. E. M., Nielander H. B., Vos J. P., Lopes da Silva S., Verhaagen J., Oestreicher A. B., Schrama L. H., Schotman P. and Gispen W. H. (1989) Expression of growth-associated protein B-50 (GAP43) in dorsal root ganglia and sciatic nerve during regenerative sprouting. *J. Neurosci.* **9,** 3505–3512.
58. Van Lookeren Campagne M., Dotti C. G., Jap Tjoen San E. R. A., Verkleij A. J., Grispen W. H. and Oestreicher A. B. (1992) B-50/GAP-43 localization in polarized hippocampal neurons *in vitro*—an ultrastructural quantitative study. *Neuroscience* **50,** 35–52.
59. Van Lookeren Campagne M., Dotti C. G., Verkleij A. J., Gispen W. H. and Oestreicher A. B. (1992) B-50/GAP-43 localization on membranes of putative transport vesicles in the cell body, neurites and growth cones of cultured hippocampal neurons. *Neurosci. Lett.* **137,** 129–132.
60. Van Lookeren Campagne M., Oestreicher A. B., Buma P., Verkleij A. J. and Gispen W. H. (1991) Ultrastructural localization of adrenocorticotrophic hormone and the phosphoprotein B-50/growth-associated protein 43 in freeze-substituted, lowicryl HM20-embedded mesencephalin central gray substance of the rat. *Neuroscience* **42,** 517–529.
61. Van Lookeren Campagne M., Oestreicher A. B., VanDerKrift T. P., Gispen W. H. and Verkleij A. J. (1991) Freeze-substitution and Lowicryl HM20 embedding of fixed rat brain—suitability for immungold ultrastructural localization of neural antigens. *J. Histochem. Cytochem.* **39,** 1267–1279.
62. Verhaagen J., Hermens W. T. J. M. C., Oestreicher A. B., Gispen W. H., Rabkin S. D., Pfaff D. W. and Kaplitt M. G. (1994) Expression of the growth-associated protein B-50/GAP43 via a defective herpes-simplex virus vector results in profound morphological changes in non-neuronal cells. *Molec. Brain Res.* **26,** 26–36.
63. Verhaagen J., Van Hooff C. O. M., Edwards P. M., De Graan P. N. E., Oestreicher A. B., Schotman P., Jennekens F. G. I. and Gispen W. H. (1986) The Kinase C Substrate Protein B-50 and Axonal Regeneration. *Brain Res. Bull.* **17,** 737–741.
64. Verkade P., Oestreicher A. B., Verkleij A. J. and Gispen W. H. (1995) The increase in B-50/GAP-43 in regenerating rat sciatic nerve occurs predominantly in unmyelinated axon shafts: a quantitative ultrastructural study. *J. comp. Neurol.* **356,** 433–443.
65. Wiedenmann B. and Franke W. W. (1985) Identification and localization of synaptophysin, an integral membrane glycoprotein of Mr 38,000 characteristic of presynaptic vesicles. *Cell* **41,** 1017–1028.
66. Woolf C. J., Reynolds M. L., Chong M. S., Emson P., Irwin N. and Benowitz L. I. (1992) Denervation of the motor endplate results in the rapid expression by terminal Schwann cells of the growth-associated protein-GAP-43. *J. Neurosci.* **12,** 3999–4010.

(*Accepted* 12 *October* 1995)